

International Journal of Modern Physics D  
 © World Scientific Publishing Company

## Swift highlights and flares (Back to the drawing board?)

G. Chincarini,<sup>1,2</sup> R. Margutti,<sup>1,2</sup>

<sup>1</sup> *Dipartimento di Fisica “G. Occhialini”, Università Statale di Milano Bicocca, Piazza della Scienza 3, I-20126 Milano, Italy.*

<sup>2</sup> *INAF - Osservatorio Astronomico di Brera, via Emilio Bianchi 46, I-23807 Merate (Lc), Italy.  
 E-mails: guido.chincarini@brera.inaf.it, raffaella.margutti@brera.inaf.it.*

Swift opened up a new era in the study of gamma-ray burst sources (GRB). Among a variety of discoveries made possible by Swift, here we focus on GRB 090423, the event at  $z=8.2$  which currently holds the record of the most distant celestial object ever caught by human instrumentation. This GRB allowed us to have a direct look at the early Universe. The central engine activity giving origin to the GRB emission is also discussed starting from the observational findings of an updated GRB X-ray flares catalog.

*Keywords:* Gamma-ray bursts; gamma-ray sources; gamma-rays.

### 1. Introduction

Each time we build and use innovative state of the art instrumentation we expect to detect new phenomena and details that allows a better understanding of the physics of the objects we are observing. In the case of the Swift mission<sup>8</sup> we were able to build on the experience obtained by Beppo-Sax and on the theoretical developments that helped the design allowing targeting critical points of the GRB physics. The result was a multi-wavelength mission with very fast pointing, accurate astrometry of the transients and real time analysis and communication of the detected targets.

Out of the variegated science and related high lights we have recently published, here we will discuss GRB 090423, a burst holding the high  $z$  record for any celestial object so far discovered, and illustrate some of the results we obtained with the new sample of GRB flares. In other words we will look into the early Universe and perhaps into the activity intimately related to the central engine.

Nowadays we have evidence that the early star formation, pop III, is followed by the re-ionization (of HI) phase that likely terminated at  $z \sim 6$ . As it is well known even a small amount of neutral hydrogen would heavily absorbs at wavelengths smaller than  $\text{Ly}_\alpha$  (Gunn - Peterson effect) so that this region in which some neutral hydrogen still exist in the IGM is easily recognizable and indeed it is a powerful tool to track down the various phases of the process as a function of redshift.

2 *G. Chincarini, R. Margutti*

In the X-ray light curve of the afterglow (generally covering the temporal range of few hundreds second since trigger to a million second after that) we define as flare an event that manifests itself as a sudden change in the observed flux and lasting a time largely smaller than the light curve of the GRB itself. The cause of these later injections of energy is not yet known and while it may be caused either by late shocks among shells emitted during the prompt emission or, more likely, by renewed activity of the central engine, they are certainly not due to external shock (it can be shown that the pulse width divided by the time of occurrence of the pulse is too small to be explained as due to external shock). But no matter what, a clear understanding of the observed emission will lead to the understanding of the mechanism at work and eventually lead to the understanding of the central engine. Any correlation among parameters of flares occurring at different time in different bursts must relate to a behavior of the central engine and may lead to its partial understanding.

## 2. The re-ionization epoch and GRB 090423

Following the formation of neutral and molecular hydrogen (the cosmic abundance is that determined by the primordial nucleosynthesis) the formation of the Pop III stars reionizes the intergalactic medium. Information about this important phase of the cosmic evolution comes from the objects observed at very high  $z$ . High  $z$  objects (the search of high  $z$  objects has been an observational game since ever) can be detected using various techniques and various dedicated surveys, among these the fundamental Hubble Space Telescope Ultra Deep Field survey and the SDSS have lead to fundamental results. For  $z > 5$ , the drop out technique<sup>23</sup> using multi filters optical observations is the least biased and likely gives the strongest indication for a spectroscopic follow up. One of the major goal justifying the search of high  $z$  galaxies is, in addition to the understanding of the formation and evolution of Pop III stars, the understanding of the sources that reionize the observations at that epoch (for a brief and clear description of the problem see Ref. 21 and references therein). The most distant galaxy has been detected at  $z = 6.96$ <sup>13</sup> while the most distant AGN has been detected at  $z \sim 6.43$ <sup>29</sup>. Photometric indications (these galaxies and AGN are too faint to get a spectrum even with the very large telescopes) exist of objects with  $7 < z < 10$ ; what is really needed is the spectrum in order to have not only a certain identification but also the possibility to measure continuum and lines to estimate the population and the metal abundance.

In the last few years, and this was one of the goals of the Swift mission, the GRBs came into the game. Their very large luminosity makes them visible and detectable at very high  $z$  and the featureless power law spectrum of the afterglow make of them an ideal beacon to identify the absorption lines of the ISM of host galaxy and the characteristics of the IGM with the advantage on the AGN of not being affected by the proximity effect. There is always a price to pay and that is

due to the rapid decay of the luminosity so that we must target them soon after the detection of the prompt emission. To this end the technology is at hand however; we need to build 3 to 4 meters aperture robotic telescopes with state of the art focal plane instruments<sup>28,4</sup>.

Swift detected three objects for which the optical follow up evidenced through their spectra very high  $z$  objects: GRB 050904 at  $z = 6.29$ <sup>10</sup>, GRB 080913 at  $z=6.7$ <sup>9</sup> and GRB 090423 at  $z = 8.2$ <sup>20,24</sup>. The latter hold the record for any celestial object so far observed.

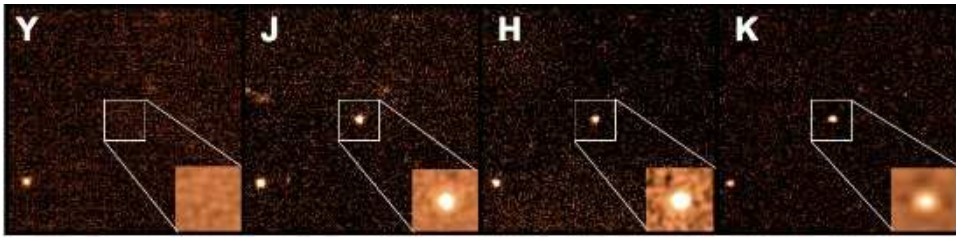


Fig. 1. These images obtained with the UKIRT telescope in Hawaii clearly indicate the GRB had to be at high  $z$ . The  $Ly_{\alpha}$  break (12.15 nm) is located between the Y filter (120 nm) and the J filter (213 nm);  $z > 7.5$ . Using the 4 filter it is possible, however, to estimate a reasonably good redshift. (Courtesy of N. Tanvir)

It is only matter to look at the GCN sequence to partially reconstruct the way the two teams arrived at the spectroscopic detection of the redshift. While most of the data were kept confidential it was clear that the lack of detection at certain wavelengths and the identification of the object at higher wavelengths, we reproduce in Figure 1 the best photometric sequence obtained with the UKIRT telescope in Hawaii, indicated that we were certainly dealing with a very high  $z$  object. In Italy we were able to trigger the TNG after we had long discussions about the Nature of the event and after getting the first spectrum (14 hours after the burst) we recall that the next day during the Swift teleconference we stressed we were checking the data and preparing a second GCN. The two groups had the first evidence that objects, stars producing GRBs, indeed exist at those redshifts and that the search for such objects near the dawn of the epoch of the formation of the first stars was fully justified.

The host galaxy of GRB 050904<sup>1</sup> indicate a mass smaller than a few  $10^9$  solar masses while the metal lines<sup>10</sup> call for a rather low metallicity  $Z \sim 0.05Z_{\odot}$ .

Unfortunately the spectrum of GRB 090423 does not show any detectable emission or absorption line due to the very small signal to noise ratio. Our spectrum,

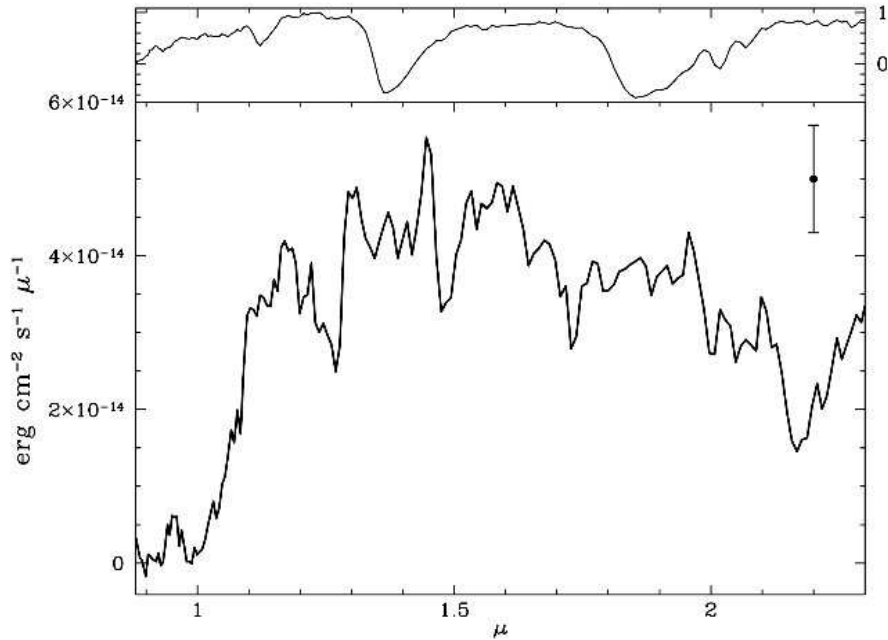
4 *G. Chincarini, R. Margutti*

Fig. 2. Spectrum obtained at the Italian 3.6 m aperture TNG telescope using a de amici prism. On top the standard star that shows we are quite sensitive below 100 nm as well. Note that the de mici prism has been designed in order to have a good coverage over a large band of NIR wavelength and this is extremely useful in these cases.

obtained about 14 hours since trigger, was obtained with a 3.6 meter telescope while the spectrum obtained by the Tanvir group using the VLT (8.2 meter aperture) was gathered at later times in the bands  $0.98 - 1.1 \mu\text{m}$  and  $1.1 - 1.4 \mu\text{m}$  respectively. We also attempted to use the X ray spectrum to estimate the metal content of the host galaxy using the absorption edge of the X ray spectrum. However these measures, even if indicative, are rather uncertain both because of the need to disentangle various effects (response matrix, variability, power law spectrum etc.) and because the interpretation is not unambiguous (absorption systems along the line of sight). The somewhat astonishing result we derive especially from the X ray light curve of the afterglow and from the radio observations is that the high  $z$  GRB afterglow is completely similar to the long GRBs we observed at low redshift.

The Radio afterglow<sup>5</sup> furthermore enable a better estimate of the isotropic (jet) gamma-ray energy  $E_\gamma \sim 10^{53}$  erg ( $> 2.2 \cdot 10^{51}$  erg) and a blast wave kinetic energy  $E_K \sim 3.8 \cdot 10^{53}$  erg ( $> 8.4 \cdot 10^{51}$  erg). At high  $z$  we seem to detect the very bright end of the GRB luminosity distribution function and it seems that the progenitors are the same.

### 3. Flares

The discovery of flares, given the previous observations with Beppo-SAX and the light curves of the first GRBs detected by Swift, came to the Swift team as one of the biggest surprises to the extent that we also discussed the possibility they could be an artifact of the instrument.

Their understanding are of paramount importance because a) they reflect brief and powerful injection of energy that must likely be related to the central engine, b) they have been detected both in long and short GRBs indicating a mechanism that must be the same in both types of events. The open questions are many and it is not yet clear whether we have all the observations we need to answer them. The observed X-ray light curve shows a number of features that are not fully accounted by the standard (internal - external shock) model. The spectrum of the prompt emission may include a thermal component and in any case being rather flat below the peak does not fit the synchrotron emission, the afterglow light curve presents an yet unexplained plateau that either requires a large injection of energy or may be related to an external shock with very high energy budget however. Often (see for instance GRB 070110<sup>26</sup>) a very steep drop follows that may be eventually related to combined flare activity.

In GRB 080319B (the naked eye GRB<sup>19</sup>) we observed rapid variability both at high energy and in the optical, Figure 3. The optical light curve variability on a scale of 5 to 10 s follows with a delay of about 6 seconds relative to the hard X ray variability while differences exist (here however it is essential to plan for higher time resolution at optical wavelengths) at higher frequency variability. Even invoking an inverse Compton for the high-energy emission the differences in variability and the delay call for a revised model.

The short GRBs present in some cases light curves of the afterglow that are similar to those of the long GRBs; in some cases the prompt emission present an extended tail that may eventually call for a new classification. The morphology long short is related to the general consensus that short GRBs are due to the merging NS+NS and long to the collapse of a massive star. A long lasting prompt emission for a short may be at variance with the timing of the phenomenon or with the source of the accreted material. If the additional emission during the early phase is due to a left over of the merging<sup>27</sup> then we may have a late accretion that should be however present in most of the observed shorts. The afterglow light curve, see for instance GRB 050724, is often similar and presents a steep decay, plateau and further decay. In these cases is the phenomenology exactly the same, environment included, independently of the progenitor?

Long and short GRBs present flares in their light curve. This sudden and brief

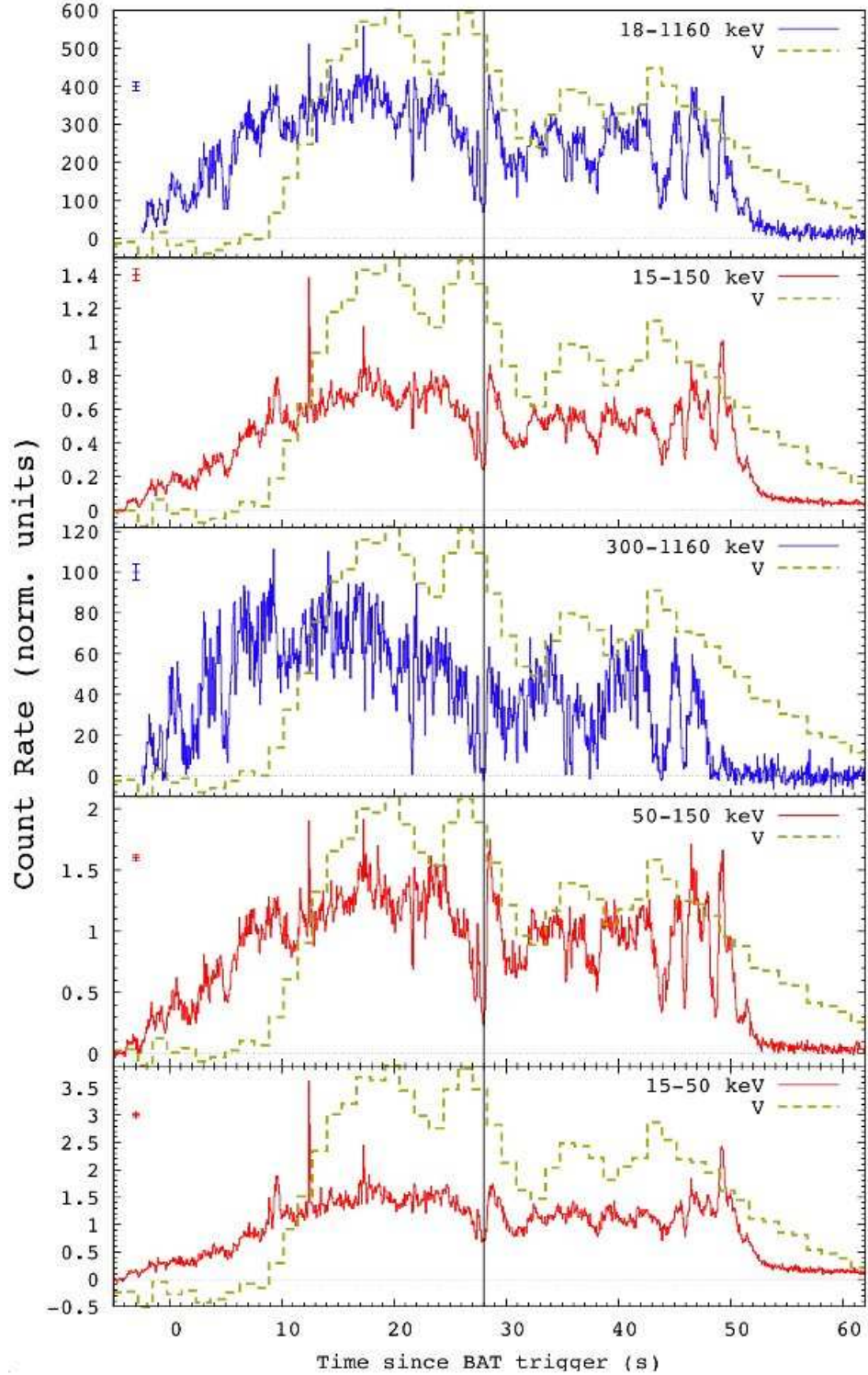
6 *G. Chincarini, R. Margutti*

Fig. 3. The continuous lines in blue and red are the observations obtained by the Konus - Wind satellite and Swift BAT. The yellow in the optical by the TORTORA camera mounted on the REM Telescope. Courtesy of C. Guidorzi.

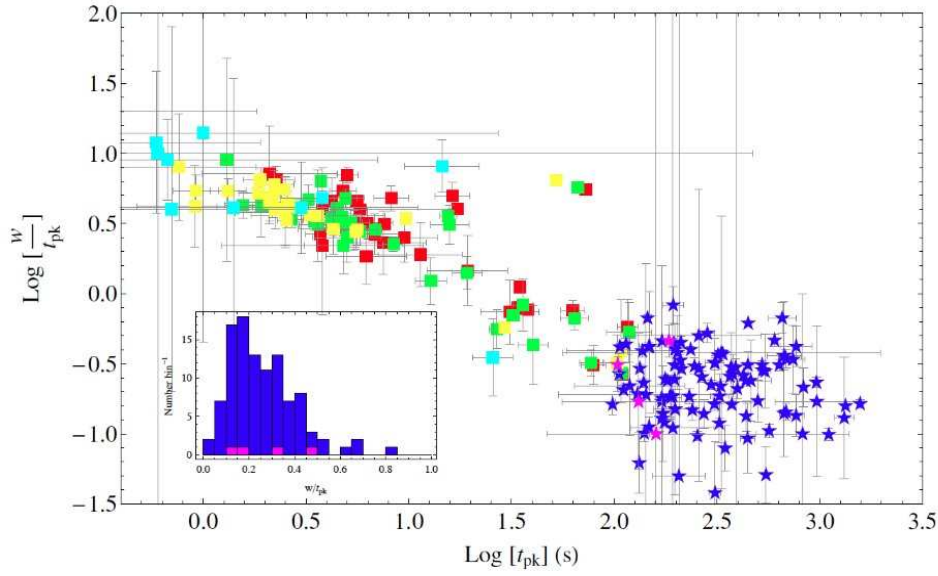


Fig. 4. Width to  $t_{peak}$  ratio as a function of  $t_{peak}$ , (blue stars). The squares refer to the BATSE pulses measured by Ref. 16 and the different colors to different energy channels. In the inset we have the distribution of the ratio with the red color referring to the flares observed in short GRBs.

injection of energy that can occur at any time during the afterglow may help in determining the mechanism of emission and the characteristics of the central engine. In a simple minded model the observed width to peak ratio ( $\Delta t/t \sim 0.2$ ) call for a radius of emission of about  $10^{17}$  cm that is too large to be produced by internal shock when compared to the deceleration radius,  $R \sim \left( \frac{E_K}{\gamma_0 n m_p c^2} \right)^{1/3} \sim 10^{17}$  cm. We almost completed the analysis of a new sample of 113 X-ray flares, 43 of which have a measured redshift. The sample was analyzed in 5 XRT bands (0.3 keV - 10 keV, 0.3 keV - 1 keV, 1 keV - 2 keV, 2 keV - 3 keV and 3 keV - 10 keV) in order to measure some parameters as a function of energy. The net result of this analysis<sup>4,15,2</sup> is that we confirm previous results<sup>3,6</sup> and give more evidence that the flares observed during the afterglow have the same characteristics of the pulses observed in the low luminosity (see the distribution function in Ref. 18) GRBs. In Figure 4 we plot in conjunction of the XRT flares the pulses observed during the prompt emission phase<sup>16</sup>. There is continuity with a smooth transition from the prompt emission to the afterglow flares with the difference however that while the observed prompt emission pulses maintain a constant width, the width of the XRT flares increase with time.

Of outmost importance is the energy budget. The sample is not complete and we did not push the identification for very faint flares since one of the constraints we had in the sample was to be able to measure the profile. Flares are very energetic and represent bursts of energy of about 10% the energy the energy emitted during

8 *G. Chincarini, R. Margutti*

the afterglow. In a few cases, GRB 050502B is the prototype, the energy emitted during the flare is about the whole energy emitted during the afterglow. Late flares show a smaller amplitude and a much larger width, the energy however does not change that much even if it is somewhat smaller than the energy emitted by early flares<sup>2</sup>.

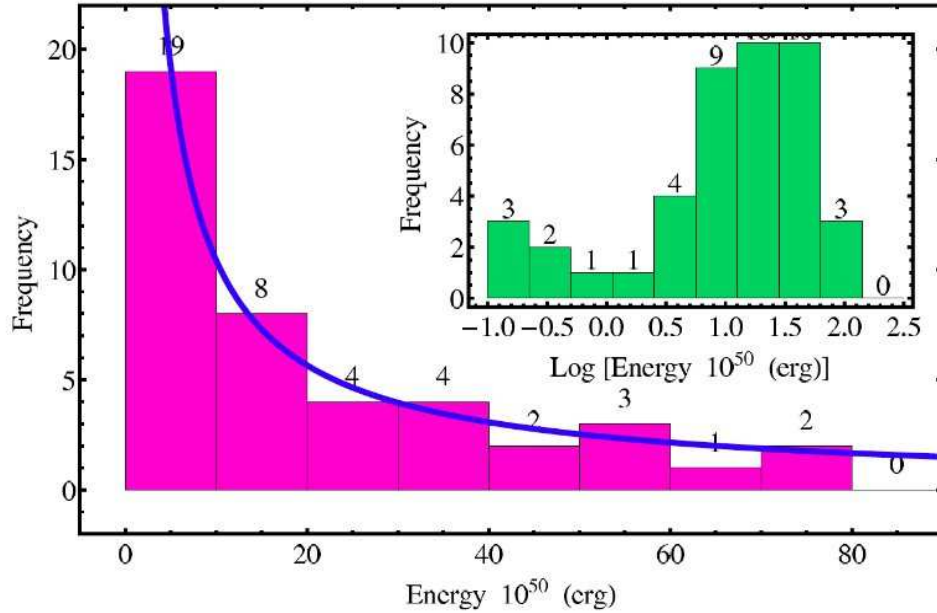


Fig. 5. Distribution of energy of flares having spectroscopic redshift. In the histogram of the inset the energy has been expressed in log units.

As for the pulses observed during the prompt emission we measure a variation of the width with energy. In this case we define an efficient energy  $E_{eff}$  as the energy weighted over the pass band by the following relation:

$$E_{eff} = (1+z) \frac{\int E f(E) RM dE}{\int f(E) RM dE} \quad (1)$$

In this way and after correcting and using the rest frame width we find a net correlation between the width and the energy of the flare: at higher energies the flares are narrower.

Indeed the correlation we find:  $w_{RF} = 10^{1.5} E_{eff}^{-0.5}$  is very similar to that estimated by Ref. 7 for pulses observed by BATSE:  $w \propto E^{-0.4}$ .



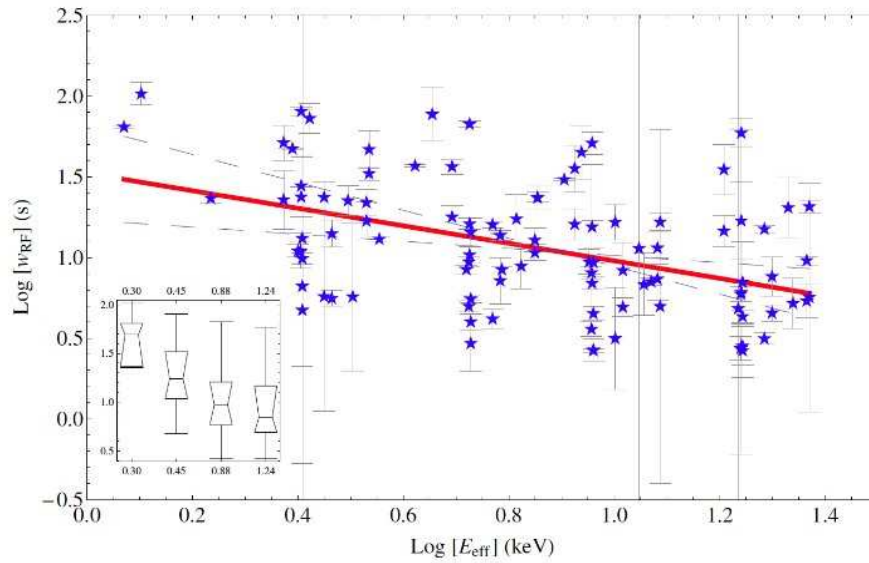


Fig. 6. Plot of the rest frame width as a function of the efficient energy. In the inset the related quantile plot.

It is remarkable that in all the correlations the flares reflect the same characteristics of the prompt emission pulses indicating a similar mechanism at work and likely the same origin so that this activity lasts from the prompt emission to about a million second after the trigger.

#### 4. Discussion and conclusions

Recent observations challenge the fireball internal shock model. Optical observations do not show strong evidence of the reverse shock<sup>11</sup>, and in any case even if present does not seem to be one of the main component of the early optical emission<sup>17</sup>. The reverse shock is weak or suppressed in the magneto hydro dynamical models of GRBs<sup>25,22,14</sup> so that the goal is to find way to estimate whether  $\sigma_0 = \frac{F_p}{F_b} = \frac{B_0^2}{(4\pi\gamma_0\rho c^2)}$  is  $\gg 1$  (the jet is dominated by a Pointing flux) or  $\ll 1$  (the kinetic energy of the baryonic jet dominates).

We should add incidentally, that the mechanism by which strong magnetic fields and the acceleration of particles to very high energy is achieved is not yet fully known. It needs to be demonstrated that the linear Fermi mechanism is capable of doing the job following the back and for transit of the particles in the shock region.

To summarize part of the results in a diagram we refer to plot of the ratio  $\Delta F/F$

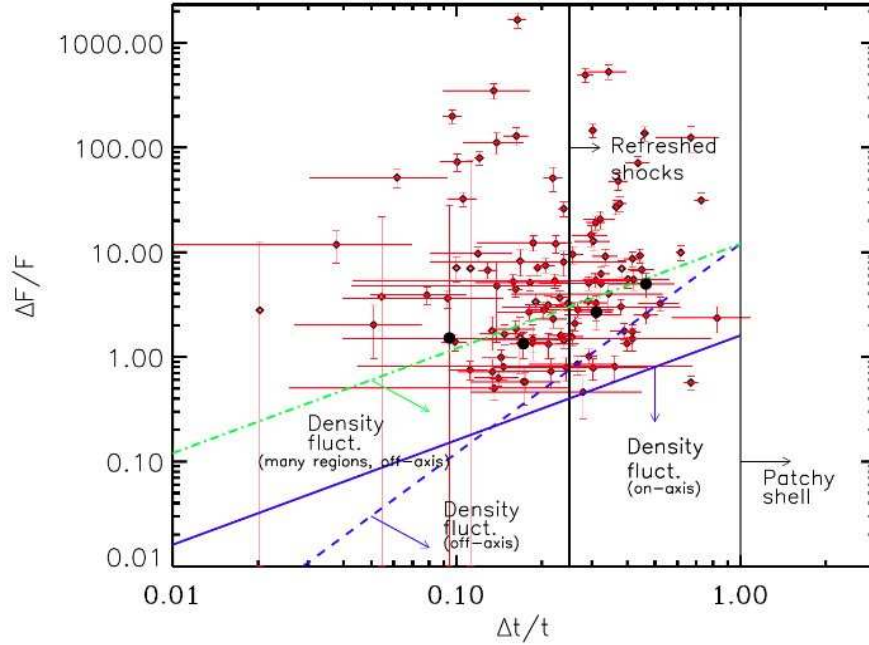


Fig. 7. The relative variability of the flares as a function of the width to time ratio has been plotted. The limits shown by the various lines have been calculated according to the equations given in Ref. 12. The 4 black dots refer to short GRBs.

versus  $\Delta t/t$ , Figure 7. Here  $\Delta F$  is the variation of the flux above the underlying continuum over the flux observed in the underlying continuum and  $\Delta t/t$  the flare width over the time of the peak of the flare.

The complete absence of flares with  $\Delta t/t > 1$  confirms that flares cannot be due to patchy shells. Flares furthermore seem to have a high probability, as expected, to be observed off axis and a large number of flares would, according to this plot, agree with the refreshed shock model.

Flares are not necessarily the result of late central engine activity, but may be produced in the decelerating phase of the flow. High  $\sigma_0$  values may lead to MHD instabilities during the interaction with the interstellar medium. In this case the isotropic equivalent energy emitted in a single flare and produced by a single reconnection event, is related to the ratio width/ $t_{peak}$  by the relation:

$$E_{flare} \leq 5 \epsilon \left( \frac{width}{t_{peak}} \right)^3 \frac{E_{forward shock}}{\alpha^2} \quad (2)$$

where  $\epsilon \sim 0.1$  and  $\alpha$  in the range 2 - 4 depending on the density of the ISM. The flares we observe are not in contradiction within errors with this relation but, at the same time, they do not prove it.

In conclusion we find that flares seem to retain memory of the previous event so that, as time progresses, each flare is weaker and softer of the preceding one. And finally while we are making significant progress in characterizing these events observationally, at the moment there is no satisfactory model explaining their origin, evolution and energetics.

### Acknowledgments

This work is supported by ASI grant SWIFT I/011/07/0, by the Ministry of University and Research of Italy (PRIN, MIUR, 2007TNYZXL), by MAE and by the University of Milano Bicocca (Italy).

### References

1. Berger, E. et al. *ApJ* **665** (2007) 102
2. Bernardini, M. et al. *MNRAS* (2010) submitted
3. Chincarini, G. et al. *ApJ* **671** (2007) 1903
4. Chincarini, G. et al. *MNRAS* (2010) submitted
5. Chandra, P. et al. *ApJ* **712** (2010) L31
6. Falcone, A.D. et al. *ApJ* **671** (2007) 1921
7. Fenimore, E.E. *ApJ* **448** (1995) L101
8. Gehrels, N. et al. *ApJ* **611** (2004) 1005
9. Greiner, J. et al. *ApJ* **693** (2008) 1610
10. Kawai, N. et al. *Nature* **440** (2006) 184
11. Kumar, P.; McMahon, E.; Panaitescu, A. et al. *MNRAS* **376** (2007) L57
12. Ioka, K. et al. *ApJ* **631** (2005) 429
13. Iye, M. et al. *Nature* **443** (2006) 186
14. Lyutikov, M. and Blandford, R. *ArXiv 0312347* (2003)
15. Margutti, R. et al. *MNRAS* (2010) submitted
16. Norris, J.P. et al. *ApJ* **627** (2005) 324
17. Oates, S.R. et al. *MNRAS* **395** (2009) 490
18. Quilligan, F. et al. *A&A* **385** (2002) 377
19. Racusin, J. et al. *Nature* **455** (2008) 183
20. Salvaterra, R. et al. *Nature* **461** (2009) 1258
21. Salvaterra, R. et al. *MNRAS* submitted (2010), *ArXiv 1003.3873*
22. Spruit, H.C. et al. *A&A* **369** (2001) 694
23. Steidel, C.C. *Ap.J.* **462** (1996) L17
24. Tanvir, N. et al. *Nature* **461** (2009) 1254
25. Thompson, C. *MNRAS* **270** (1994) 480
26. Troja, E. et al. *ApJ* **665** (2007) 599
27. Troja, E. et al. *MNRAS* **401** (2009) 1381
28. Vitali F. et al., *SPIE Astronomical Telescopes and Instrumentation: Observational Frontiers of Astronomy for the New Decade*, Vol.**7733**(2010)
29. Willott, C.J. et al. *AJ* **14** (2007) 2435